

Crossing and duality consistent study of Λ , Σ^0 , and $\Lambda(1405)$ production by kaon photoproduction and radiative capture

Robert A. Williams, Chueng-Ryong Ji, and Stephen R. Cotanch

North Carolina State University, Raleigh, North Carolina 27695

(Received 15 October 1990)

We report a comprehensive analysis of the crossing related reactions $p(\gamma, K^+)Y$ and $p(K^-, \gamma)Y$ for $Y = \Lambda$, Σ^0 , and $\Lambda(1405)$. Our model, which incorporates both crossing and duality, reproduces all existing Λ and Σ^0 cross-section, polarization, and capture branching-ratio data while providing useful constraints for the $\Lambda(1405)$ magnetic transition moments. While the $p(\gamma, K^+)\Lambda(1405)$ cross section is predicted to be measurable at CEBAF ($\sigma \sim 1 \mu\text{b}$), parity conservation leads to a model-independent suppression of the $p(\gamma, K^+)\bar{\Lambda}(1405)$ polarization and $p(K^-, \gamma)\Lambda(1405)$ cross section ($\sigma \sim 1 \text{ nb}$).

Since the early 1960's several phenomenological studies have been separately conducted on kaon photoproduction and radiative capture.^{1,2} However, these analyses did not incorporate crossed-channel data which provides an important, fundamental constraint on the model parameters.³ We have recently reported⁴ a crossing-consistent analysis which produced an improved set of coupling constants that now simultaneously describe the available data for both the photoproduction $p(\gamma, K^+)\Lambda$ and capture $p(K^-, \gamma)\Lambda$ reactions. That analysis utilized a fairly elaborate pole model containing 12 tree-level diagrams. However, without additional phenomenological input, the previous analysis cannot be directly applied to other production or capture channels, including the $\Lambda(1405)$. In this paper we employ a duality constraint to develop a more restricted model which comprehensively describes the crossing-related kaon photoproduction and radiative capture reactions for Λ and Σ^0 production and which also provides a realistic prediction for $\Lambda(1405)$ production. Such a model is important because of the keen interest in electromagnetic processes involving production of the complete hyperon spectrum.

The duality constraint required in this analysis is based on the dual role of resonances in the $s(u)$ and t channels. Dolen, Horn, and Schmid⁵ have shown that so-called interference models, which include resonances in both channels simultaneously, produce an overcomplete (double-counting) description of the amplitude. Renard and Renard⁶ used the finite-energy sum rule (FESR) for the kaon photoproduction process and showed that their low-energy amplitude including s - and u -channel resonances (not including t -channel K^*-K^{**} resonances) reproduces well on the average the features of the high-energy amplitude based on Reggeized K^* and K^{**} exchange. Therefore, we consider only s - and u -channel resonances along with the usual Born graphs (including p in the s channel, Σ^0 and Λ in the u channel, and, for gauge invariance, the K^+ exchange in the t channel). Since the t -channel (K^*) exchanges are not included by duality, we avoid problems at higher energies associated with the tensor coupling of non-Reggeized K^* exchanges.⁷ Hence we have more confidence in our

$\Lambda(1405)$ predictions [$\Lambda(1405)$ production has a threshold at $E_\gamma = 1.45 \text{ GeV}$, an energy where other models start to fail]. Because calculations^{8,9} have demonstrated that the $\Lambda(1405)$ dominates the capture width, we include it as a resonance in the u channel. Two N^* resonances contribute in the s channel, the $N_- \equiv N(1650)$ and $N_+ \equiv N(1710)$, having opposite parities and significant decay fractions into $K^+\Lambda$ and $K^+\Sigma^0$. Our model is minimal in the sense that we include only the necessary spin- $\frac{1}{2}$ intermediate-state diagrams to produce a reasonable description of available Λ and Σ^0 data. This minimal model is attractive since it contains fewer parameters than in previous analyses, but is able to describe more data. We neglect the low-lying spin- $\frac{1}{2}$ N^* resonances because in the kinematic range of interest ($0.9 \leq E_\gamma \leq 2.0 \text{ GeV}$) these virtual states are nonresonant and are much farther off their mass shell. Thus there are a total of seven distinct diagrams for each hyperon reaction [except for Σ^0 production where we also include two Δ graphs: $\Delta_- \equiv \Delta(1620)$ and $\Delta_+ \equiv \Delta(1910)$]. A single, effective coupling constant can be associated with each diagram defined to be the product of the strong and electromagnetic vertex couplings that are listed in Table I.

Our basic philosophy differs from other approaches which do not utilize crossing symmetry or duality, but do stress coupling-constant constraints determined by phenomenological analyses of purely hadronic reactions.^{2,7,10} We agree that it is highly desirable to develop a model which can successfully describe both electromagnetic and hadronic processes with one common set of parameters.¹¹ However, we submit that it is inconsistent to directly apply parameters determined by hadronic investigations to electromagnetic studies when the two analyses differ significantly in both theoretical concept and computational accuracy (the purely hadronic treatments use dispersion relations, whereas the electromagnetic descriptions employ a perturbative diagrammatic approach). Therefore, until a more ambitious model is developed which treats hadronic and electromagnetic reactions within the same, consistent formalism, we advocate that electromagnetic applications should use parameters

TABLE I. Strong and electromagnetic coupling constants used in this analysis. Numbers in parenthesis are an alternative set of values used to establish the theoretical uncertainty in the $\Lambda(1405)$ production cross section. Note that the extracted effective coupling constants referred to in the text are $G \equiv \mu g$.

| Strong | Electromagnetic (μ_B) |
|---|--|
| $g_{KN\Lambda} = 4.127$ | $\mu_p = 1.793$ |
| $g_{KN\Sigma^0} = -0.329$ | $\mu_\Lambda = -0.613$ |
| $g_{KN\Lambda(1405)} = 1.5 (3.0)$ | $\mu_{\Sigma^0} = 0.81$ |
| $g_{KN_+\Lambda} = 6.393$ | $\mu_{\Lambda(1405)} = 0.44$ |
| $g_{KN_-\Lambda} = 0.81$ | $\mu_{\Sigma^0\Lambda} = 1.61$ |
| $g_{KN_+\Sigma^0} = 9.08$ | $\mu_{\Lambda(1405)\Lambda} = -0.224 (-0.112)$ |
| $g_{KN_-\Sigma^0} = 0.332$ | $\mu_{\Lambda(1405)\Sigma^0} = 1.077 (0.538)$ |
| $g_{KN_+\Lambda(1405)} = g_{KN_-\Lambda}$ | $\mu_{N-p} = 0.406$ |
| $g_{KN_-\Lambda(1405)} = g_{KN_+\Lambda}$ | $\mu_{N+p} = 0.097$ |

determined comprehensively, and exclusively, from processes with constraints imposed from crossing and duality, but not the hadronic sector.

Because our model does not include the parameters associated with t -channel (K^*) exchanges, we can now simultaneously describe all three Λ , Σ^0 , and $\Lambda(1405)$ reaction channels in kaon photoproduction, $p(\gamma, K^+)Y$, and the crossing related radiative capture, $p(K^-, \gamma)Y$, processes. The Λ , Σ^0 , and $\Lambda(1405)$ photoproduction (capture) reactions are interrelated and complementary because the amplitude for each process involves diagrams with different combinations of the same strong and electromagnetic coupling constants. All of the coupling constants except $g_{KN\Lambda(1405)}$, $g_{KN_+\Lambda(1405)}$, and $g_{KN_-\Lambda(1405)}$ are first determined phenomenologically by the Λ and Σ^0 processes, and are then used to predict the $\Lambda(1405)$ amplitudes. The $\Lambda(1405)$ anomalous magnetic moment is computed theoretically from both an SU(3) quark model and a hadronic $\bar{K}N$ wave function [we use the $\bar{K}N$ value for consistency with the SU(3)-violating transition moments]. The two hadronic $KN_\pm\Lambda(1405)$ coupling constants are determined by the chiral symmetry of the Lagrangian including $g_{KN_+\Lambda}$ and $g_{KN_-\Lambda}$. For $g_{KN\Lambda(1405)}$, which is not uniquely determined, we use the value obtained from hadronic scattering (~ 3.0) as an upper bound and show the sensitivity of our $\Lambda(1405)$ results to this parameter. The resulting coupling constants generate a good description of all available Λ and Σ^0 production cross-section and polarization data, while predicting capture branching ratios within the error of the new experimental values.¹² The Born couplings are primarily constrained by the Λ data, being much less sensitive to the Σ^0 data, which is mainly responsible for fixing the $KN^*\Sigma$ and $K\Delta\Sigma$ couplings. It should be noted that the values we obtain for $g_{KN\Lambda}$, G_{N_+} , and G_{N_-} are substantially different by a factor of 2–20 from the values obtained in recent photoproduction analyses. However, these differences are not surprising since no other analysis incorporates crossing and duality constraints in a minimal model. The small $g_{KN\Lambda}$ is a direct consequence of the du-

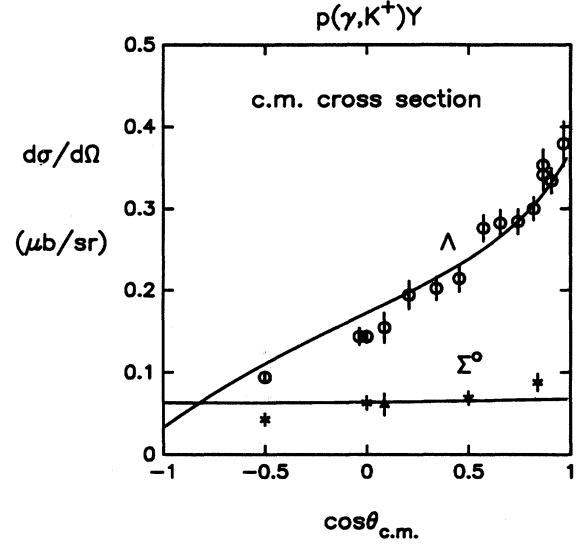


FIG. 1. Photoproduction angular distributions for Λ at $E_\gamma = 1.2$ GeV and Σ^0 at $E_\gamma = 1.1$ GeV.

ality constraint since t -channel graphs (which are excluded in this model) are known¹⁰ to produce interference with the Born terms which enhance $g_{KN\Lambda}$. The difference of a factor of 20 in G_{N_+} and G_{N_-} couplings is not unreasonable because the effective N^* couplings are very uncertain in all models.

Figure 1 is representative of our global χ^2 fit and illustrates the angular distributions for $p(\gamma, K^+)Y$ at 1.2 GeV for Λ and at 1.1 GeV for Σ^0 . Note in Fig. 2 the energy dependence of the Σ^0 cross-section data, suggesting an important resonance contribution near $\sqrt{s} \sim 1.9$ GeV.

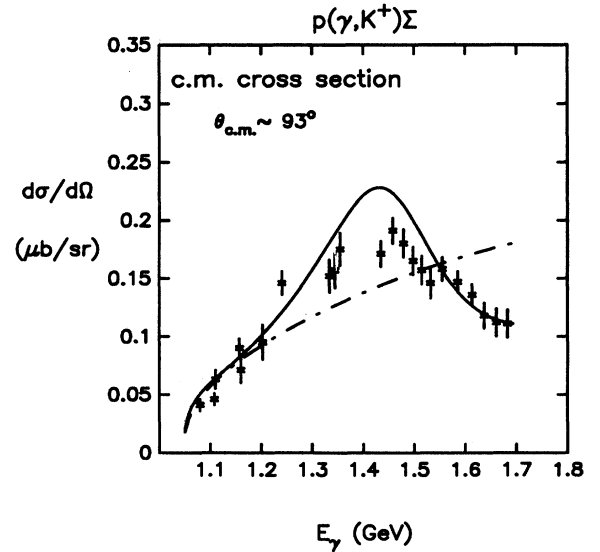


FIG. 2. Energy dependence of $p(\gamma, K^+)\Sigma^0$ at $\theta_{c.m.} \sim 93^\circ$. Solid line represents full Δ result. Dot-dashed line represents the no- Δ result.

This energy behavior can only be reproduced, in part, by our model if the $\Delta(1620)$ and $\Delta(1910)$ isobars are included (the solid line represents the full Δ calculation, while the dash-dot-dashed line represents the no Δ result). In view of the magnitude of this effect, it is interesting to note that the Δ diagrams have only a small effect on the Σ^0 capture branching ratio. Since isospin conservation forbids Δ contributions to Λ and $\Lambda(1405)$ production, Σ^0 photoproduction appears to offer the only opportunity to study this effect and additional, more accurate measurements are strongly recommended. In Fig. 3 we plot the Λ and Σ^0 polarization at 90° as a function of the laboratory photon energy. In contrast to the Λ , the Σ^0 polarization is negative, and while there is currently no data to confirm this prediction, it is interesting that in purely hadronic production measurements for $p + {}^9\text{Be} \rightarrow Y + X$, opposite Λ and Σ^0 polarizations, are observed.¹³ Another key result is a new, improved value for the ratio of $\Lambda(1405)$ electromagnetic transition moments, $R = \mu_{\Lambda(1405)\Lambda} / \mu_{\Lambda(1405)\Sigma^0}$. By exploiting the capture branching-ratio sensitivity to the transition moment and incorporating recent experimental limits on the branching ratios, we have obtained a more stringently bound ratio $R = -0.21 \pm 0.08$. This small, negative ratio severely violates the SU(3) prediction $R = +\sqrt{3}$ [broken flavor SU(3) predicts an even larger ratio $R = (3)^{3/2} M_s / (2M_s + M_u)$, where M_u and M_s are the up- and strange-quark masses, respectively], and clearly implies that the $\Lambda(1405)$ may not be the SU(3) singlet ground state. Further, because there are no other Σ^* or N^* states with similar mass and parity, the $\Lambda(1405)$ cannot be included in an SU(3) octet. These findings support the conjecture that the $\Lambda(1405)$ is not a pure three-quark system, but rather is a more complicated structure—a result consistent with the exotic $\bar{K}N$ molecular representation suggested by several authors.¹⁴⁻¹⁶ Predictions for the $\Lambda(1405)$ production cross section are plotted in Fig. 4 and contrasted with Λ production for the same incident

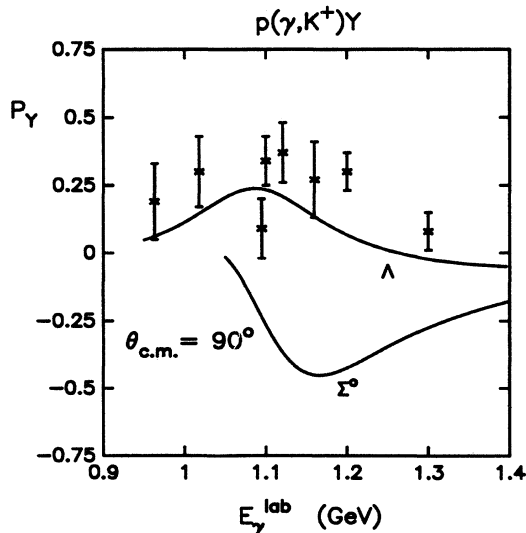


FIG. 3. Polarization of Λ and Σ^0 vs E_γ at $\theta_{\text{c.m.}} \sim 90^\circ$.

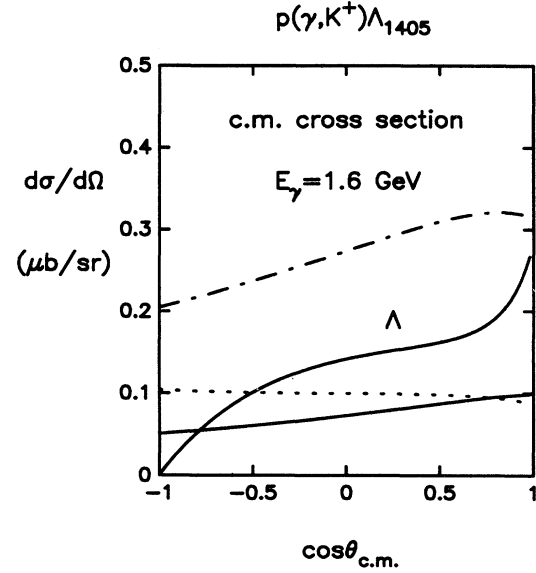


FIG. 4. Photoproduction cross section for the $\Lambda(1405)$ at $E_\gamma = 1.6$ GeV showing the sensitivity to the unconstrained parameters (solid line for $g_{KN\Lambda(1405)} = 1.5$; dot-dashed line for $g_{KN\Lambda(1405)} = 3.0$). Dotted line demonstrates sensitivity to N^* resonances ($g_{KN\Lambda(1405)} = 1.5$ and N^* coupling constants set equal to zero).

energy. This figure also demonstrates the sensitivity to the $KN\Lambda(1405)$ coupling constant, as the solid and dot-dashed curves were generated using the values of 1.5 and 3, respectively. We expect the measured cross section to lie somewhere in between these curves. The dotted line, which uses $g_{KN\Lambda(1405)} = 1.5$ and $g_{KN^\pm\Lambda(1405)} = 0$, indicates the sensitivity to the $g_{KN^\pm\Lambda(1405)}$ coupling constants. In all cases, the $\Lambda(1405)$ production distributions are roughly isotropic with a magnitude similar to the Λ cross section. The maximum $\Lambda(1405)$ polarization, however, is very small (< 0.1). Unfortunately, the $p(K^-, \gamma)\Lambda(1405)$ at rest capture branching ratio is predicted to be unmeasurable ($\sim 10^{-6}$). Figure 5 shows all of the capture cross-section predictions as a function of kaon laboratory momentum.

The large sensitivity of the $\Lambda(1405)$ photoproduction cross section to the $KN\Lambda(1405)$ coupling constant is significant and indicates that this parameter can be accurately determined when future experimental data become available. More fundamentally, this sensitivity is a natural consequence of parity conservation, which is also the reason why our model predicts a small $\Lambda(1405)$ polarization. The $\Lambda(1405)$ has negative intrinsic parity compared with the positive Λ and Σ^0 parities. Parity conservation determines which partial-wave component dominates the production amplitude (since the model contains only spin- $\frac{1}{2}$ intermediate states, angular momentum conservation permits only s and p waves to contribute). Λ and Σ^0 production are dominated by even-parity diagrams (the proton graph for Λ and the Λ graph for Σ^0) which produce substantial p -wave components in the amplitude as evidenced by the large Λ and Σ^0 polarizations. The same

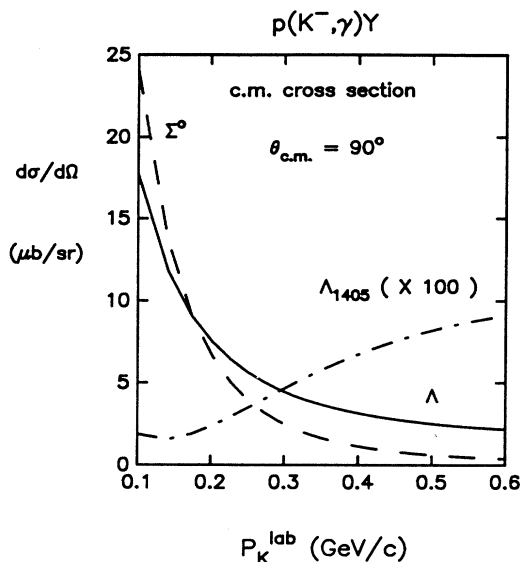


FIG. 5. In-flight capture cross sections at $\theta_{c.m.} = 90^\circ$ for Λ , Σ^0 , and $\Lambda(1405)$ as a function of the kaon laboratory momentum.

diagrams dominate $\Lambda(1405)$ photoproduction; hence parity conservation selects a large s -wave component and thereby produces a small polarization and an increased sensitivity to the proton graph. The $\Lambda(1405)$ production threshold at $\sqrt{s} \sim 1.9$ GeV is about 300 MeV away from the nearest possible resonant N^* state and about 200 MeV away from the nearest resonance below threshold; hence the small $\Lambda(1405)$ polarization is believed to be a model-independent result for photoproduction near threshold. The small capture cross section for the $\Lambda(1405)$ also follows from parity conservation combined with $\Lambda(1405)$ domination in the capture channel and the absence of other nearby u -channel Λ^* resonances. We conclude that our model provides realistic and model-independent predictions for $\Lambda(1405)$ production in both photoproduction and capture channels.

In conclusion, we have used a relativistic pole model which can be comprehensively applied to Λ , Σ^0 , and $\Lambda(1405)$ photoproduction and kaon radiative capture processes. We find that our minimal model not only works as well as our previous model⁴ for the $p(\gamma, K^+)\Lambda$ and $p(K^-, \gamma)\Lambda$ reactions, but also has the added features of successfully describing the Σ^0 photoproduction and radiative capture data and providing useful predictions for the $\Lambda(1405)$ processes. Low-energy production of the $\Lambda(1405)$ is found to be very small in the capture channel [$\sigma \sim 1$ nb for $K^-p \rightarrow \gamma\Lambda(1405)$], whereas in photoproduction it is comparable with the Λ and Σ^0 ($\sigma \sim 1$ μ b). This is a model-independent result which follows from parity conservation. Hence low-energy studies of $\Lambda(1405)$ formation should be more feasible in the (γ, K^+) channel. At higher energies (e.g., for K^- momentum above ~ 0.6 GeV/c), the $\Lambda(1405)$ in-flight capture cross section may be significantly enhanced by excited hyperon resonances [such as $\Lambda(1600)$, $\Sigma(1660)$, etc.] to permit production studies at kaon factories. Utilizing the capture branching-ratio sensitivity to the $\Lambda(1405)$, Λ , and Σ^0 transition moments, new phenomenological limits have been established for the transition moment ratio $R = -0.21 \pm 0.08$, a value that severely violates the SU(3) prediction $R = +\sqrt{3}$. We believe this is further phenomenological support for the claim that the $\Lambda(1405)$ may not be a pure three-quark state. Clearly, more experimental data is needed to test this model. Obviously, an electroproduction study would be complimentary and provide additional constraints on this model. We are currently pursuing an analysis of the available electroproduction data [which includes limited $\Lambda(1405)$ production data] to further test and develop this model.

Financial support from the U.S. Department of Energy grant DE-FG05-88ER40461 and DE-FG05-90ER40589 is gratefully acknowledged. We also acknowledge the North Carolina Supercomputing Center for the grant of Cray Y-MP time.

¹S. Hatsukade and H. J. Schnitzer, Phys. Rev. **128**, 468 (1962); **132**, 1301 (1963); M. Gourdin and J. Dufour, Nuovo Cimento **27**, 1410 (1963); T. K. Kuo, Phys. Rev. **129**, 2264 (1963); **130**, 1537 (1963); H. Thom, *ibid.* **151** 1322 (1966); K. H. Larsen and S. R. Deans, Bull. Am. Phys. Soc. **15**, 182 (1969); W. Schorsch, J. Tietge, and W. Weilnbock, Nucl. Phys. **B25**, 179 (1970); F. M. Renard and Y. Renard, Nucl. Phys. **B25**, 490 (1971); R. A. Adelseck *et al.*, Phys. Rev. C **32**, 1681 (1985); R. L. Workman and H. W. Fearing, Phys. Rev. D. **37**, 3117 (1988).

²Most recent calculations including polarized target experimental data are given in R. L. Workman, Phys. Rev. C **40**, 2922 (1989); R. A. Adelseck and B. Saghai, *ibid.* **42**, 108 (1990).

³C.-R. Ji and S. R. Cotanch, Phys. Rev. C **38**, 2691 (1988).

⁴R. A. Williams, C.-R. Ji, and S. R. Cotanch, Phys. Rev. D **41**, 1449 (1990).

⁵R. Dolen, Horn, and Schmid, Phys. Rev. Lett. **19**, 402 (1967); Phys. Rev. **166**, 1768 (1968).

⁶F. M. Renard and Y. Renard, Nucl. Phys. **B25**, 490 (1971); Y.

Renard, *ibid.* **B40**, 499 (1972).

⁷H. Tanabe *et al.*, Phys. Rev. C **39**, 741 (1989).

⁸Y. S. Zhong *et al.*, Phys. Rev. D **38**, 837 (1988).

⁹Jurij W. Darewych *et al.*, Phys. Rev. D **32**, 1765 (1985).

¹⁰C. Bennhold and L. E. Wright, Phys. Rev. C **39**, 927 (1989).

¹¹J. Cohen, Phys. Lett. B **192**, 291 (1987); **153B**, 367 (1985); Phys. Rev. C **32**, 543 (1985); **39**, 2285 (1989).

¹²D. A. Whitehouse *et al.*, Phys. Rev. Lett. **63**, 1352 (1989).

¹³E. Leader, in *Intersections Between Particle and Nuclear Physics (May 26-31, 1986, Lake Louise, Canada)*, Proceedings Conference on Intersections Between Particle and Nuclear Physics, edited by D. F. Geesaman, AIP Conf. Proc. No. 150 (AIP, New York, 1986), p. 257.

¹⁴R. H. Dalitz and S. F. Tuan, Phys. Rev. Lett. **2**, 425 (1959); Adelseck and Wright, Phys. Rev. C **38**, 1965 (1988).

¹⁵J. J. Sakurai, Ann. Phys. (N.Y.) **11**, 1 (1960); R. C. Arnold and J. J. Sakurai, Phys. Rev. B **12**, 2808 (1962).

¹⁶E. A. Veit *et al.*, Phys. Lett. **137B**, 415 (1984); E. A. Veit *et al.*, Phys. Rev. D **31**, 1033 (1985); **31**, 2242 (1985).